Automatic urban trees detection from airborne LiDAR data using 3D descriptor and intensity

Cleber Junior Alencar[1], Mauricio Galo[2], Renato César dos Santos[2]

[1]Sao Paulo State University – UNESP, Graduate Program in Cartographic Sciences, Presidente Prudente, São Paulo – Brazil – cleber.alencar@unesp.br
[2]Sao Paulo State University – UNESP, Dept. of Cartography, Presidente Prudente, São Paulo – Brazil – mauricio.galo@unesp.br, renato.cesar@unesp.br

Keywords: Urban forests, Point cloud processing, LiDAR, Photogrammetry, Remote sensing.

Abstract

Urban trees play an important role for improving city liveability, as they help reduce heat, air pollution, flood risk, while supporting a balanced and sustainable microclimate. Thus, detecting and monitoring urban trees are vital for the effective management and environmental conservation of cities. Traditional remote sensing methods rely on imagery from optical sensors, but they face limitations in capturing inner tree structural information. In this context, LiDAR (Light Detection And Ranging) data can be a suitable alternative. Although point-cloud based approaches explore directly the three-dimensional (3D) information inherent in raw LiDAR data, the effectiveness of 3D descriptors and intensity values for tree detection remains underexplored, particularly in heterogenous urban environments with mixed trees compositions. This work introduces an automatic and unsupervised approach for urban tree detection from airborne LiDAR data, combining intensity information with the omnivariance, a 3D descriptor calculated from eigenvalues. A two-step K-means clustering method is applied – first to identify potential tree points using intensity, then to detect actual trees using the omnivariance feature – followed by morphological guided filtering to reduce misclassification. The tests were carried out on six different areas selected in datasets from Brazil and New Zealand. The evaluation was based on manually labelled reference data. The obtained results reveal an overall accuracy of 89% and low omission errors (6%), indicating method's robustness across varied urban scenarios.

1. Introduction

Urban trees are essential for improving city liveability, as they help to reduce heat island effects, mitigate air pollution, reduce flood risk, maintain the microclimate balance and promote a sustainable urban development (Zhang et al., 2022). In this sense, the detection and monitoring of trees in urban areas have increasingly become a key component for city management and for an effective environmental governance by public authorities. Additionally, tree detection and crown delineation contribute to optimize buildings and power line detection algorithms, as these objects are often occluded by tall trees (dos Santos et al., 2022; Munir et al., 2023). Within this context, the development of effective methods for tree detection can be vital for urban planning, ensuring infrastructure maintenance, and supporting the conservation of urban environments.

Traditional remote sensing methods for detecting trees usually rely on bidimensional (2D) data such as optical images from aerial and/or orbital platforms. With the LiDAR (Light Detection And Ranging) technology advancement with the growing availability of data, new approaches have been proposed to expand its potential application, particularly in the context of urban forests. This can be ascribed to LiDAR system's capacity to acquire a large amount of three-dimensional (3D) data with high accuracy, obtained directly from the integration of GNSS (Global Navigation Satellite System), IMU (Inertial Measurement Unit) and LASER (Light Amplification by Stimulated Emission of Radiation) scanning unit. Moreover, depending on the tree structure, LiDAR pulse can penetrate small gaps in the crown and reach branches, trunks, and the ground bellow the vegetated areas, which enables to retrieve tree's inner structure information. Thus, it is possible to use this data to estimate important metrics such as height, crown height and diameter, canopy area and volume, as well as to estimate biomass and carbon stock (Zhang et al., 2022).

Methods focused on tree detection from LiDAR data can be categorized into two main groups: image-based and point-based. Image-based methods rasterize the original point cloud creating a Canopy Heigh Model (CHM) and use traditional image processing algorithms, including watershed segmentation, region growing, graph-cut segmentation, which are more suitable to delineate trees in 2D space and for species classification (Jia et al., 2025). Point-based strategies, in turn, draw on geometric 3D descriptors derived from the point cloud and clustering algorithms (Alencar et al., 2023; Singh and Yadav, 2023; Liu et al., 2025). Also, intensity values stored with each LiDAR point can potentially be explored in tree detection (Budei et al., 2022; Kashani et al., 2015).

While image-based algorithms perform well in detecting dominant trees, the process of rasterization causes loss of substantial vertical information that could be used to identify subdominant trees, especially in complex forest environments (You et al., 2021; Liu et al., 2024). In addition, machine learning and deep learning strategies, especially semi-supervised or supervised approaches, require a training step, and it can be challenging to obtain high-quality samples that represents all the complexity of the urban environment (Hao Liu et al., 2025).

Although more robust methods have been proposed to detect trees effectively, they are generally applied to native and planted forests (Hao Liu et al., 2025), and largely rely on geometric characteristics of forests (dos Santos et al., 2024). Nevertheless, tree detection in urban environments is still challenging due to their structural complexity, where various infrastructure elements frequently coexist with vegetation, and trees of different species, crown densities, sizes and spatial distribution. Also, the intensity information can be assessed more thoroughly.

This contribution has been peer-reviewed. The double-blind peer-review was conducted on the basis of the full paper.
https://doi.org/10.5194/isprs-annals-X-3-W4-2025-15-2026

In this context, this paper proposes an automatic point-based method for urban trees detection using LiDAR data acquired by one Airborne LASER Scanning (ALS) platform. The method combines intensity information and the 3D descriptor omnivariance, based on the local eigenvalues, to classify tree and non-tree points using the unsupervised classifier K-means. Additionally, a classification refinement is proposed based on mathematical morphology. The results from six different areas in two countries are compared to reference point clouds classified manually for each sub-set to assess the method effectiveness in terms of precision, recall and *F-score*.

2. Proposed Method

Figure 1 illustrates the proposed method's workflow. Basically, it includes outlier detection; identification of potential tree points using intensity values; detection of tree points using 3D descriptor (omnivariance); and a classification refinement guided by mathematical morphology.

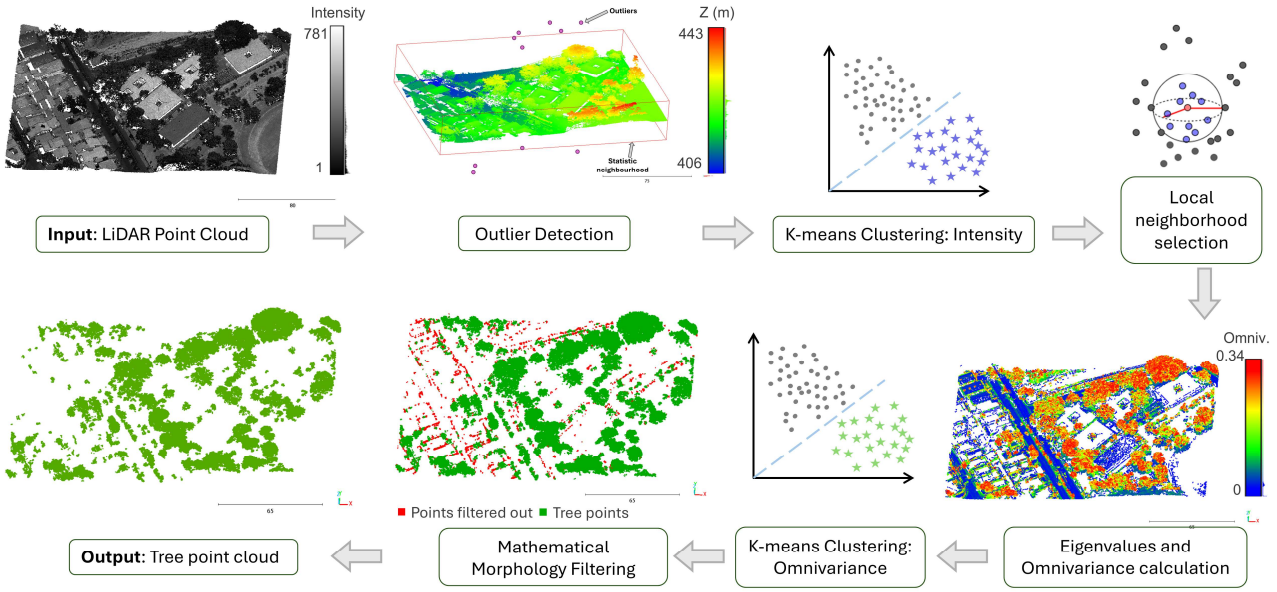

Figure 1 - Representation of the proposed method for tree detection.

2.1 Outlier Detection

A preprocessing step was performed to remove potential outliers from the point clouds. According to Shiffler (1988), outliers can be defined as a value that exceeds 3 or 4 standard deviations from de mean. In Carrilho and Galo (2017), the proposed method considers any point in the point cloud an outlier if its altitude (Z coordinate) falls out of a predefined range based on the mean ($\bar{z}$), standard deviation (σ_z) and an arbitrary value (n). Therefore, this same approach was adopted in this study and the range of inliers was defined as:

$$[\bar{z} - n\,\sigma_z;\ \bar{z} + n\,\sigma_z]. \quad (1)$$

Following the same concept, an outlier detection was proposed for the intensity values as well. According to Kashani et al. (2015), this information is also susceptible to unexpected measurements caused by several parameters related to both LiDAR system and data acquisition geometry. Thus, Equation 1 can be rewritten as:

$$[0;\ \bar{I} + n\,\sigma_I]. \quad (2)$$

Note that intensity values cannot be negative, so the lower bound is set to 0 (zero).

Initially, the mean and the standard deviation for both Z coordinate and intensity were calculated for the entire point cloud. Then, each point was evaluated whether its Z coordinate fell within the defined interval bounds. Points identified as outliers were excluded from the point cloud. Finally, the same procedure was applied to the intensity values. However, in this case outliers were not removed but instead, replaced by the upper bound value of the respective interval. This approach was adopted to avoid the loss of a potential points and still mitigate the influence of anomalous values.

2.2 Identification of potential tree points using intensity

The intensity value of LiDAR represents the energy of the LASER pulse reflected by each target and depends on the object's surface material and reflectivity properties. Consequently, the reflected signal may produce higher or lower intensity value, depending on the spectral and geometric properties of the object. According to Wehr and Lohr (1999), objects like asphalt and concrete are expected to have less than 30% of reflectivity, while snow and white masonry bricks can have more than 80% of reflectivity, considering a near infrared pulse. Particularly for trees, the reflectivity is attenuated due to their dossel rugosity that reflects the LASER pulse to different directions besides the system detectors.

As observed in Alencar et al. (2023), the intensity values associated with trees are mainly distinct from those of buildings, ground surfaces and sidewalks, but tend to be similar to roads. Based on this distinction, an initial classification process was carried out using K-means clustering, leveraging intensity to separate the point cloud into two classes: potential tree points and non-tree points. The benefits of using K-means clustering for LiDAR point classification have been validated in prior studies

This contribution has been peer-reviewed. The double-blind peer-review was conducted on the basis of the full paper.
https://doi.org/10.5194/isprs-annals-X-3-W4-2025-15-2026 | © Author(s) 2026. CC BY 4.0 License.

(dos Santos et al., 2022; Alencar et al., 2023; dos Santos et al., 2024). The K-means algorithm allows the point cloud to be partitioned into a predefined number of K classes based on selected features similarity, such as intensity, spatial distribution or geometric descriptors.

2.3 Detection of tree points using 3D descriptor

Using the potential tree points detected in the first step, the second classification was carried out based on the local 3D descriptor. Given a local neighbourhood of a point i, the eigenvalues $(\lambda_1, \lambda_2, \lambda_3)$ were calculated from the local 3D variance-covariance matrix, where $\lambda_1 \geq \lambda_2 \geq \lambda_3 \geq 0$. These eigenvalues were used to compute omnivariance (Equation 3).

$$O_{\lambda_i} = \sqrt[3]{\lambda_1\ \lambda_2\ \lambda_3}. \quad (3)$$

According to Weinmann et al. (2015), this feature describes how the points are arranged locally in terms of spatial distribution. The more scattered the points are in the neighbourhood, the higher is the omnivariance value.

A spherical neighbourhood with radius (r) equal to 1 m was defined for each point i in the potential tree point cloud, and the omnivariance was subsequently computed. The choice of neighbourhood was guided by the findings of a study conducted by Alencar et al. (2023), where different types and sizes of neighbourhood were analysed along with other 3D descriptors. In the context of tree point detection, the use of a spherical neighbourhood presented promising performance.

For the proposed method, the potential tree point cloud obtained in a previous step (Section 2.2) was classified using K-means and omnivariance. Two classes were then created: tree points and non-tree points.

2.4 Refinement based on mathematical morphology

It is known that some points with high elevation from the ground, such as those from poles, power lines and roof edges, can often be misclassified as trees by point-based algorithms (You et al., 2021; Alencar et al., 2023). Then, the refinement process aimed to remove those points is applied. In our study, the proposed strategy is divided into three steps: binary grid generation; MM-guided filtering; and 3D point cloud reconstruction.

2.4.1 Grid generation

To enable the application of MM filter, a regular grid was created based on the following steps:

1. Generate a regular grid with a predefined cell size (s_{grid});
2. For each grid cell center, identify the nearest point from the tree point cloud using a 2D distance threshold (t_{xy});
3. Assing a value to the cell: 1 (one) when a tree point is located and 0 (zero) when no point is located (empty cell).

This procedure resulted in a binary image representing the spatial distribution of the two classes (tree and non-tree). The cell size can directly affect the final results; therefore, the size defined in this work considered the average point spacing (ps_{avg}) of the dataset. The planar distance threshold $t_{xy,}$ as well, was set by the same value.

2.4.2 MM-guided filtering

After, a MM filter is applied to the binary image generated in the previous step (2.4.1). Since misclassified points are predominantly sparse, a morphological opening operation was performed to remove isolated points, linear structures and small clusters (Figure 2).

Morphological opening is an MM operation that consists of the application of erosion followed by a dilation, using one given structuring element (*se*) for both operators. The erosion step removes pixels and shrinks objects to remove small noise components. Subsequently, the dilation operator restores shape and size of the remaining structures. In this work, a disk with radius (d_r) of size two grid pixels was defined as the *se*, in proportion to the size and shape of tree crowns. The *se* was systematically translated pixel by pixel across the input image, and the opening operator was applied. The resulting output values were then stored in a new image, as shown in Figure 2c.

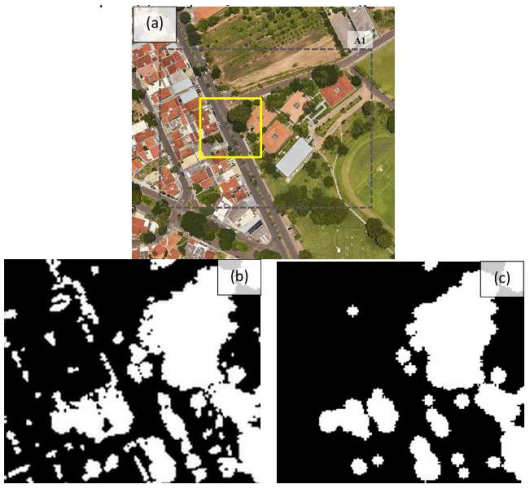

Figure 2 - Example (a) illustrating the results of the tree detection approach before (b) and after (c) MM filtering.

2.4.3 3D point cloud reconstruction

MM-guided filtering resulted in a binary image, where the pixels with the value 1 represented a tree point. For this reason, a reconstruction procedure was required to retrieve the corresponding 3D point cloud. This process followed the same logic from the previous steps; however, the filtered image served as the reference. Each point position in the initial point cloud was evaluated by examining the corresponding pixel in the filtered image: if the pixel value was 1, the point was labelled as tree; otherwise, it was labelled as a non-tree. Finally, the tree points were detected.

3. Experiment Design and Quality Assessment

3.1 Study areas and datasets

The experiments were conducted on airborne LiDAR datasets from two different locations: Presidente Prudente/Brazil (Tommaselli et al., 2018) and Palmerston North/New Zealand (OpenTopography, 2020). In order to cover a broader diversity of urban scenarios, three different areas were selected from each dataset to evaluate the method's performance (Figure 3).

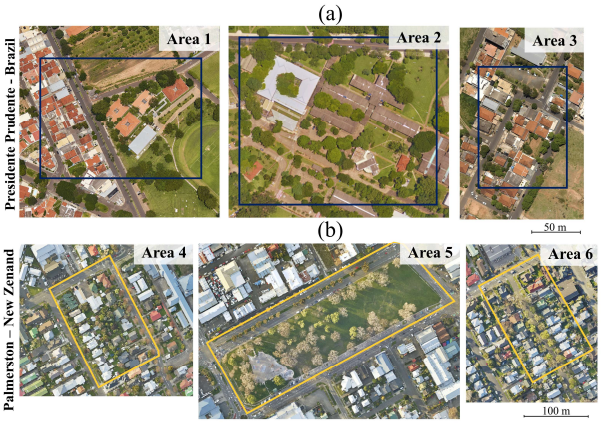

Figure 3 - Study areas from Presidente Prudente/Brazil dataset (a) and from Palmerston North/New Zealand dataset (b).

The areas selection was based on their diversity of trees, structure patterns and density of vegetation, as well as the presence of typical urban objects (buildings, cars, power lines, walls and poles). Table 1 presents some information about each dataset used, and their respective study areas selected.

	LiDAR Dataset	
	Presidente Prudente/Brazil	Palmerston/New Zealand
Study areas	1, 2 and 3	4, 5 and 6
LiDAR system	LMS-Q680i	Orion H300
Average Point Spacing (m)	0.4	0.2
Average Point Density (pts/m²)	12	22

Table 1 – Datasets information.

3.2 Performance assessment

Both qualitative and quantitative evaluations were performed to assess the proposed method effectiveness. The automatic tree detection results were compared to reference data generated manually by visual interpretation of high-resolution images.

Quantitative assessment was carried out by computing three quality indicators (Equations 4-6): completeness (*Comp.*), correctness (*Corr.*) and *F-score*. These metrics are widely used in point classification studies (Sokolova et al., 2006; Chen et al., 2018; dos Santos et al., 2024) and they range from 0 to 1, where values closer to 1 indicate a positive match between the results and the reference data.

$$Comp. = TP/(TP + FN) \quad (4)$$

$$Corr. = TP/(TP + FP) \quad (5)$$

$$F - score = 2TP/(2TP + FP + FN) \quad (6)$$

In these equations, true positive (TP) is the number of tree points correctly detected. False negative (FN) represents the number of tree points missed by the proposed method and false positive (FP) is the points misclassified as tree. A planar distance threshold ($d_{xy} = 2 * ps_{abv}$) was set to validate a point whether to be TP, FP or FN.

3.3 Parameters settings

Table 2 summarizes the parameters involved in the tree detection method and their corresponding values adopted in the conducted experiments. In this table is possible to observe that some parameters were set according to the average point spacing ($\boldsymbol{ps_{avg}}$) of each point cloud and the smallest tree crown size intended for detection. The remaining (n and r) were defined based on previous work and empirical tests on our dataset.

Parameters	Description	Value
$\boldsymbol{ps_{avg}}$	Average point spacing. Depends on the dataset.	0.4 m and 0.2 m
$\boldsymbol{n}$	Scalar value to define range of inliers points – a higher value leads to inclusion of more points.	$n = 4$
$\boldsymbol{r}$	Search radius size for local neighbour definition.	$r = 1\,m$
$\boldsymbol{s_{grid}}$	Grid cell size of the binary image for mathematical morphology.	$s_{grid} = ps_{avg}$
$\boldsymbol{t_{xy}}$	Planar distance to identify the nearest point to the grid cell centre.	$2 * ps_{avg}$
$\boldsymbol{se}$	Structure element (disk) size. It is associated with the smallest tree crown intended to detect.	$2\ pixels$ $(= 2 * ps_{avg})$

Table 2 - Parameters and respective values adopted in the proposed method.

4. Results

The proposed method was applied to the selected areas (A1, A2, A3, A4, A5 and A6 – Figure 3) and the results are shown in Figure 4. Green points represent the detected trees. Table 3 summarizes the metrics obtained by comparing the results with the reference data.

Study Areas	*Comp.* (%)	*Corr.* (%)	*F-score* (%)
A1	94.42	81.22	87.01
A2	97.70	94.55	96.09
A3	96.13	81.98	88.28
A4	76.37	85.27	80.57
A5	97.67	96.22	96.94
A6	96.92	74.86	84.47
Mean	**93.20**	**85.68**	**88.89**

Table 3 - Quality metrics for the study areas.

5. Discussion

Figure 4 illustrates the tree detection results for all six study areas. Visual analysis indicates that the method proposed in this paper yielded consistent results in the task of tree detection, given that a significant number of tree points were successfully identified with an average completeness of 93.20%. However, misclassification still occurred due to the commission and omission errors, as highlighted in Figure 5.

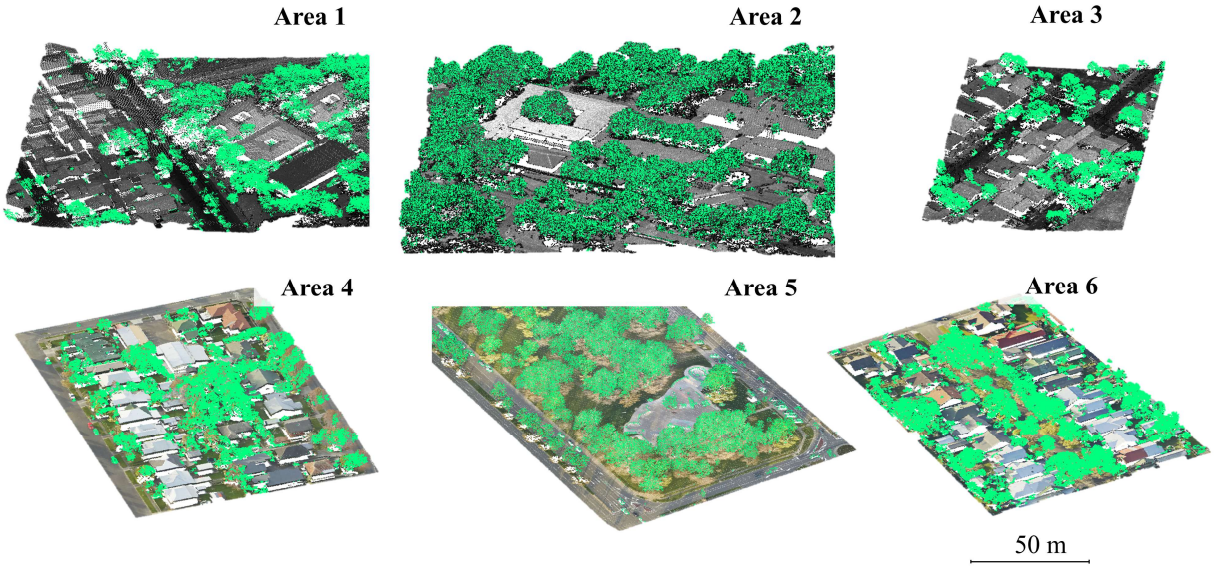

Figure 4 - Tree detection results across the six study areas.

Notably, completeness outperformed correctness (Table 3) for all the study areas since FP occurred more frequently than the FN. This suggests a tendency to confuse certain objects with trees, specially building edges and cars, leading to an increase in FP s (Figure 5). For this reason, areas A2 and A5 resulted in the highest correctness values, probably because they contained fewer buildings, while A4 and A6 underperformed. Similarly, You at al. (2021) and Alencar et al. (2023) noticed the same tendency in their methods.

Regarding to completeness, the detection approach produced remarkable results indicating that most part of the tree points were identified. On average, only 6% omission error occurred in the Presidente Prudente/Brazil dataset. On the other hand, FN were also found, especially in areas A4 and A6 from the Palmerston North/New Zealand dataset, where parts of tree crowns were neglected by the classifier.

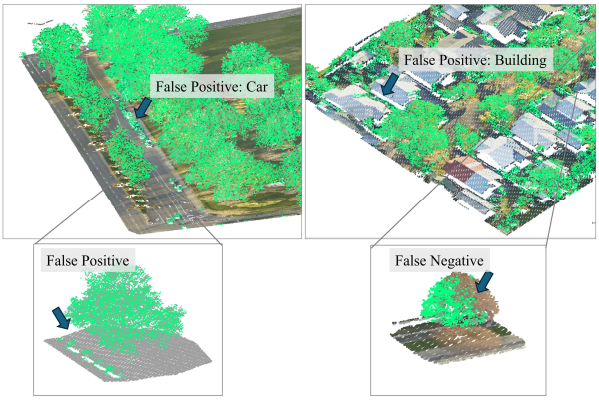

Figure 5 - Examples of false positives and false negatives in tree detection.

An important result is the potential for detecting tree points based on intensity information. This step enhanced the method's ability to detect trees, as most tree points were correctly identified, despite some non-tree points being included. In addition, the overall accuracy represented by *F-score* shows the robustness of the proposed methods to deal with different scenarios of tree occurrence and spatial distribution.

When compared with the quality metrics achieved in other studies (Table 4), the proposed method shows consistent performance. However, it is important to highlight the difference between the study areas used: some related works used planted or coniferous trees, which are typically more regular in shape and differ significantly from those found in urban environment.

Method	Types of forests	Point density (pts/m^2)	*Comp.* (%)	*Corr.* (%)	*F-score* (%)
(Özdemir et al., 2021)	Urban	8	86.82	93.07	81.51
(Pu et al., 2023)	Planted	up to 101	99.00	99.00	99.00
(dos Santos et al., 2024)	Urban	up to 12	98.7	91.2	94.8
Proposed Method		up to 22	93.20	85.68	88.89

Table 4 - Quality metrics compared to related works.

6. Conclusions

This work proposed an unsupervised method to automatically detect urban trees on LiDAR point cloud based on intensity and the geometric feature omnivariance. Results obtained from experiments in different urban areas achieved an overall accuracy of around 89% and showed the good performance of the method to detect trees, since the omission errors were low. Qualitative analyses based on visual interpretation suggests that intensity seem to help finding potential tree points. Despite its robustness, the method presented some limitations, including commission errors (particularly along building edges), as well as the uncertainty of optimal parameters setting. Future investigations will investigate the performance of the proposed method across different and larger datasets, varying the point density and location, as well as the implementation of individual tree extraction, aiming to estimate tree structural variables.

Acknowledgements

The authors gratefully acknowledge Sensormap Geotecnologia for collecting and providing Presidente Prudente/Brazil dataset;

OpenTopography for providing Palmerston North/New Zealand dataset. In addition, the authors are also thankful for the support of Coordenação de Aperfeiçoamento de Pessoal de Nível Superior – CAPES and Conselho Nacional de Desenvolvimento Científico e Tecnológico – CNPq (grant 132843/2020-0 and 309734/2022-3).

References

Alencar, C.J., Galo, M., Santos, R.C.D., 2023. Uso de Descritores 3D e Intensidade na Detecção de Árvores em Ambiente Urbano por meio de Dados LiDAR. Rev. Bras. Cartogr. 75. https://doi.org/10.14393/rbcv75n0a-63073.

Budei, B.C., St-Onge, B., Fournier, R.A., Kneeshaw, D., 2022. Effects of Viewing Geometry on Multispectral Lidar-Based Needle-Leaved Tree Species Identification. Remote Sens. 14, 6217. https://doi.org/10.3390/rs14246217.

Carrilho, A. C.; Galo, M. Remoção de Pontos Espúrios em Dados LiDAR Aerotransportado a Partir da Análise Estatística das Altitudes. *Simpósio Brasileiro de Geomática*, p. 323–327, 2017.

Chen, Wei, Hu, X., Chen, Wen, Hong, Y., Yang, M., 2018. Airborne LiDAR Remote Sensing for Individual Tree Forest Inventory Using Trunk Detection-Aided Mean Shift Clustering Techniques. Remote Sens. 10, 1078. https://doi.org/10.3390/rs10071078.

dos Santos, R.C., da Silva, M.F., Alencar, C.J., Galo, M., 2024. Automatic Detection of Trees using Airborne LiDAR Data Based on Geometric Characteristics. ISPRS Ann. Photogramm. Remote Sens. Spat. Inf. Sci. X-3–2024, 109–115. https://doi.org/10.5194/isprs-annals-X-3-2024-109-2024.

dos Santos, R.C., Habib, A.F., Galo, M., 2022. Weighted Iterative CD-Spline for Mitigating Occlusion Effects on Building Boundary Regularization Using Airborne LiDAR Data. Sensors 22, 6440. https://doi.org/10.3390/s22176440.

Jia, J., Zhang, L., Yin, K., Sörgel, U., 2025. An Improved Tree Crown Delineation Method Based on a Gradient Feature-Driven Expansion Process Using Airborne LiDAR Data. Remote Sens. 17, 196. https://doi.org/10.3390/rs17020196.

Kashani, A., Olsen, M., Parrish, C., Wilson, N., 2015. A Review of LIDAR Radiometric Processing: From Ad Hoc Intensity Correction to Rigorous Radiometric Calibration. Sensors 15, 28099–28128. https://doi.org/10.3390/s151128099.

Liu, Hao, Yang, M., Xi, B., Wang, X., Huang, Q., Xu, C., Meng, W., 2025. MFCPopulus: A Point Cloud Completion Network Based on Multi-Feature Fusion for the 3D Reconstruction of Individual Populus Tomentosa in Planted Forests. Forests 16, 635. https://doi.org/10.3390/f16040635.

Liu, Haoran, Zhong, H., Xie, G., Zhang, P., 2025. Research on Tree Point Cloud Enhancement Based on Deep Learning. Forests 16, 915. https://doi.org/10.3390/f16060915.

Liu, Y., Chen, D., Fu, S., Mathiopoulos, P.T., Sui, M., Na, J., Peethambaran, J., 2024. Segmentation of Individual Tree Points by Combining Marker-Controlled Watershed Segmentation and Spectral Clustering Optimization. Remote Sens. 16, 610. https://doi.org/10.3390/rs16040610.

Munir, N., Awrangjeb, M., Stantic, B., 2023. Power Line Extraction and Reconstruction Methods from Laser Scanning Data: A Literature Review. Remote Sens. 15, 973. https://doi.org/10.3390/rs15040973.

OpenTopography, 2020. Palmerston North, Manawatu-Whanganui, New Zealand 2018. https://doi.org/10.5069/G95B00M0.

ÖzdemiR, S., Akbulut, Z., Karsli, F., Acar, H., 2021. Automatic extraction of trees by using multiple return properties of the lidar point cloud. Int. J. Eng. Geosci. 6, 20–26. https://doi.org/10.26833/ijeg.668352.

Pu, Y., Xu, D., Wang, H., Li, X., Xu, X., 2023. A New Strategy for Individual Tree Detection and Segmentation from Leaf-on and Leaf-off UAV-LiDAR Point Clouds Based on Automatic Detection of Seed Points. Remote Sens. 15, 1619. https://doi.org/10.3390/rs15061619.

Shiffler, R.E., 1988. Maximum Z Scores and Outliers. Am. Stat. 42, 79–80. https://doi.org/10.1080/00031305.1988.10475530.

Singh, D.P., Yadav, M., 2023. 3D-MFDNN: Three-dimensional multi-feature descriptors combined deep neural network for vegetation segmentation from airborne laser scanning data. Measurement 221, 113465. https://doi.org/10.1016/j.measurement.2023.113465.

Sokolova, M., Japkowicz, N., Szpakowicz, S., 2006. Beyond Accuracy, F-Score and ROC: A Family of Discriminant Measures for Performance Evaluation, in: Sattar, A., Kang, B. H. (Eds.), AI 2006: Advances in Artificial Intelligence. Springer Berlin Heidelberg, Berlin, Heidelberg, LNCS, v. 4304, pp. 1015–1021.

Tommaselli, A.M.G., Galo, M., Dos Reis, T.T., Ruy, R. da S., Moraes, M.V.A., Matricardi, W.V., 2018. Development and Assessment of a Data Set Containing Frame Images and Dense Airborne Laser Scanning Point Clouds. IEEE Geosci. Remote Sens. Lett. 15, 192–196. https://doi.org/10.1109/lgrs.2017.2779559.

Weinmann, M., Jutzi, B., Hinz, S., Mallet, C., 2015. Semantic point cloud interpretation based on optimal neighborhoods, relevant features and efficient classifiers. ISPRS J. Photogramm. Remote Sens. 105, 286–304. https://doi.org/10.1016/j.isprsjprs.2015.01.016.

You, H., Li, S., Xu, Y., He, Z., Wang, D., 2021. Tree Extraction from Airborne Laser Scanning Data in Urban Areas. Remote Sens. 13, 3428. https://doi.org/10.3390/rs13173428.

Zhang, B., Li, X., Du, H., Zhou, G., Mao, F., Huang, Z., Zhou, L., Xuan, J., Gong, Y., Chen, C., 2022. Estimation of Urban Forest Characteristic Parameters Using UAV-Lidar Coupled with Canopy Volume. Remote Sens. 14, 6375. https://doi.org/10.3390/rs14246375.